NUMERICAL INVESTIGATION OF HEAT TRANSFER ENHANCEMENT OVER RECTANGULAR PERFORATED FIN

Kuldeep Rawat*, Ayushman Srivastav*

***Assistant Professor, Shivalik College of Engineering, Dehradun.**

Abstract

In this paper, numerical study has been performed to investigate the heat transfer and friction from a perforated fin subjected to forced convection. Thermal and fluid dynamic performances of extended surface having perforations of rectangular cross section are investigated. RANS based k–ε turbulence model is used to calculate the fluid flow and heat transfer parameters. Flow and heat transfer parameters are presented for Reynolds numbers from 2000 to 8000 based on the fin thickness. Numerical results obtained from the perforated fin geometry are compared with that of a plain fin to determine the heat transfer enhancement of test fin in extracting heat from its base under similar operating conditions.

Keywords: Perforated fin; Nusselt number; Friction factor; Reynolds number.

1. Introduction

Heat sinks are commonly used in many fields of industry as cooling electronic devices, and electronic component cooling becomes a more serious design problem as power densities continue to increase. One of the most common means for cooling electronic modules is a finned heat sink that enhances convection heat transfer to the ambient air. There are a many types of heat sinks, with differing fin geometries, and operating with forced convection but rectangular plate fins are commonly used for the reason of simplicity in manufacturing. Performance of three dimensional rectangular bluff plates or fins has been studied extensively by many investigators.

Rongguang Jia et al. [1] carried out a numerical investigation to determine the velocity and heat transfer characteristics of multiple impinging slot jets in rib-roughened channels. He considered different size and arrangement of jets and ribs and reported Results show that the ratio (B/W) between the size of the jets and ribs is most important because the ribs inhibit the motion of eddies by preventing them from coming very close to the surface when B/W is low, e.g. B/W = 1, although the ribs will increase the turbulence intensity. This blockage limited the heat transfer enhancement effect of the ribs and impinging jets. intensity. **G. Iaccarino et al. [2]** investigated the effect of thermal boundary conditions on numerical heat transfer predictions in rib-roughened passages. They obtained results using constant heat flux at the walls and conjugate heat transfer. Their experimental measurements and data correlations showed that the predicted heat transfer is very sensitive to the type of boundary conditions used in the numerical model. It was illustrated that some of the discrepancies observed between experimental and numerical data can be eliminated if conduction heat transfer in the rib is taken into account. **Meinders et al. [3]** experimentally investigated the local convective heat transfer on a wall-mounted cube placed in a developing turbulent channel flow, **Ledezma et al. [4]** performed experimental and numerical studies of heat transfer from a pin fin array heat sink in an impinging air stream. They considered pin fins with square cross section and focused on finding the optimal fin spacing. They have proposed the correlations for optimal fin-to-fin spacing and maximum thermal conductance. **Torii and Yang [5]** studied two dimensional, incompressible thermal-fluid flow over both sides of a slot-perforated flat surface, which was placed in a pulsating free stream. **Sahin and Demir [6]** experimentally investigated the variation of overall heat transfer, friction factor and effect of various design parameters on heat transfer and friction factor for a heat exchangers equipped with square cross sectional perforated pin fins in a rectangular channel. They considered effects of flow and geometrical parameters on heat transfer and friction characteristics and also obtained correlations for the efficiency enhancement. **Dorignac et al. [7]** experimentally investigated the heat transfer characteristics of a multi perforated plates. They reported that convective exchange on the upstream side of a multi perforated plate depends on the pitch between perforations. It has been concluded that the mean convective heat exchange rates around perforations can be calculated by defining the Nusselt and Reynolds numbers based on characteristics length and upstream velocity. For a large range of perforations spacing's, an empirical relation has been developed for heat exchange at windward surface of a perforated flat plate. **Shaeri et al. [8]** numerically determined the heat transfer and frictional losses from an array of solid and perforated fins mounted on a flat plate. Perforated fins have windows with square cross section and arranged in different numbers. Results showed that new perforated fins have higher total heat transfer rates with considerable weight reduction in comparison to the solid fins. It was reported that the perforated fins have relatively lesser drag and the drag ratio decreases by increasing the Reynolds number. With the increase of Reynolds number, the percentage of heat transfer enhancement with respect to solid fin depreciates in most of the cases. In a similar study, **Shaeri et al. [9]** investigated the fluid flow and convective heat transfer from an array of solid and perforated fins that are mounted on a flat plate. Perforations such as small channels with square cross section are arranged stream wise along the fin's length and their numbers varied from 1 to 3. It has been reported that fins with longitudinal pores, have remarkable heat transfer enhancement in addition to the considerable reduction in weight by comparison with solid fins.

The object of present work is to investigate the heat transfer and friction characteristics of perforated fin under forced convection using standard numerical techniques. The data pertaining to heat transfer and friction at various fluid flow rates have

been generated by solving the governing equations under the specified boundary conditions for different perforated fin geometries. The enhancement in heat transfer and friction in different cases of perforated fins are compared with that of a solid fin at different flow Reynolds number. In order to assess the heat transfer performance of the test fin, rate of heat transfer enhancement of perforated fin is determined with respect to a solid fin. Heat transfer and friction characteristics of perforated fin having different height, width and pitch of perforations are discussed with the help of relevant plots.

2. Problem description and computational domain

The computational domain chosen for a test fin is similar to the study conducted by **Shaeri et al. [9]**. The fig.1 shows a test fin attached to the base plate which is heated by providing uniform heat flux. The air flow is considered to be steady and laminar with constant properties and the air velocities are taken such that forced convection is the dominant heat transfer mechanism between perforated fin and surrounding air. The aluminium is considered as a fin material due to its suitability in the manufacturing of fins. The test fin length (L), the height (h_f) and thickness (D) are considered as 50 mm, 25mm and 5mm, respectively. The computational domain consists of an entry section, an exit section and the upper free stream surface as planes 'abcd', 'ijkl' and 'bckj', respectively. The dimensions of entrance and exit regions are kept as 15D and 30D on the upstream and downstream side of fin respectively. The domain extends twice the fin height in Y direction and 5D in Z direction. A uniform flow conditions are considered at the inlet section 'abcd' by defining the velocity components at the inlet as: $u_{in} = u_\infty$; $v_{in} = w_{in} = 0$ and $T_{in} = T_\infty$. The free stream conditions are also applied to the upper plane 'bckj'. The exit plane 'ijkl' is sufficiently far from the plate 'efgh', therefore temperature and pressure gradients are neglected along X direction. All the remaining planes are considered to be solid adiabatic walls with no slip conditions at the surfaces. The temperature of fin base plane 'efgh' (T_b) is kept 70^{o}C whereas the free stream temperature of fluid (T_∞) is considered as 25 ^{o}C.

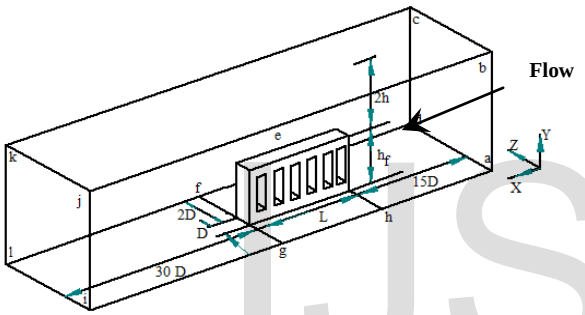

Fig.1: Computational domain.

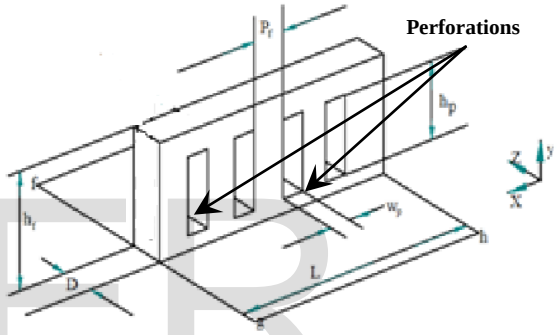

Fig.2: Perforated fin geometry.

In agreement to the observation of **Leung and Probert [10]**, the effect of radiation heat transfer is neglected for present work. The geometrical parameters of perforated fin is shown in fig.2 in which the rectangular perforations can be seen on the broad surface of the solid fin. The perforations of width (W_p) and height (h_p) are separated by perforation pitch (P_f). The relative height of perforation (h_p/h_f) is defined as the ratio of perforation height to the fin height. The width of perforation is expressed in a dimensionless form as relative perforation width (W_p/L) which is the ratio of perforation width to the fin length. The relative perforation pitch (P_f/W_p) is given as the ratio of pitch to width of perforation.

The results of grid independency study for a plain fin are shown in Table 1. It can be noticed that the insignificant changes in the values of Nusselt number and friction factor are observed due to the refinement in the grid configuration beyond the grid size of 85×33×18 for the fin and 553×102×53 for the whole domain.

Table 1: Grid independency test for a plain fin (Re = 5000).

Grids in whole domain (X×Y×Z)	Grids in plain fin (X×Y×Z)	Nusselt Number (Nu)	Friction factor (f)
275×50×20	50×25×5	20.33	0.00618
370×70×39	68×35×8	22.02	0.00580
398×73×31	73×37×9	22.24	0.00576
362×86×36	85×33×18	22.58	0.00563
553×102×53	85×33×18	22.60	0.00538
602×126×67	101×51×21	22.61	0.00533

3. Numerical method

3.1 RNG k-ε turbulent model

The RNG k-epsilon (k- ε) model is used to model the turbulent flow in the present work to compliment the conditions that the flow is incompressible with constant thermal conductivity, no heat dissipation, no compression work and no heat generation. The turbulence is assumed to be homogeneous and isotropic and therefore, the turbulence kinetic energy (*k)*, and its rate of dissipation (ε), are given by following two equations

$$\rho(\bar{u}\frac{\partial k}{\partial x}+\bar{v}\frac{\partial k}{\partial y}+\bar{w}\frac{\partial k}{\partial z})=[(\mu+\frac{\mu_t}{\sigma_k})(\frac{\partial^2 k}{\partial x^2}+\frac{\partial^2 k}{\partial y^2}+\frac{\partial^2 k}{\partial z^2})]+G_k-\rho\varepsilon \quad (1)$$

And turbulent energy dissipation rate equation is

$$\rho(\bar{u}\frac{\partial \varepsilon}{\partial x}+\bar{v}\frac{\partial \varepsilon}{\partial y}+\bar{w}\frac{\partial \varepsilon}{\partial z})=[(\mu+\frac{\mu_t}{\sigma_\varepsilon})(\frac{\partial^2 \varepsilon}{\partial x^2}+\frac{\partial^2 \varepsilon}{\partial y^2}+\frac{\partial^2 \varepsilon}{\partial z^2})]+C_{1\varepsilon}\frac{\varepsilon}{k}G_k-C_{2\varepsilon}\rho\frac{\varepsilon^2}{k} \quad (2)$$

Where G_k represents the generation of turbulent kinetic energy due to mean velocity gradients, and can be calculated using Boussinesq hypothesis as $G_k = \mu_t S^2$, where *S* is the modulus of the mean rate-of-strain tensor, defined as $S \equiv \sqrt{(2S_{ij}\, S_{ij})}$ and Sij can be defined as

$$S_{ij}=\frac{1}{2}\left(\frac{\partial \overline{u_i}}{\partial x_j}+\frac{\partial \overline{u_j}}{\partial x_i}\right) \quad (3)$$

The turbulent (or eddy) viscosity μ_t is computed by combining *k* and ε as follows:

$$\mu_t=\rho C_\mu\frac{k^2}{\varepsilon} \quad (4)$$

The model constants for the two transport equations $C_{1\varepsilon}$, $C_{2\varepsilon}$, C_μ, σ_k and σ_ε have the following values $C_{1\varepsilon}$= 1.42; $C_{2\varepsilon}$=1.68; C_μ=0.085; σ_k=1.0; σ_ε=1.3

3.2 Solution method

FLUENT 13.0 is used to solve the incompressible RANS equations using a second order upwind scheme chosen for energy and momentum equations and the SIMPLE pressure–velocity coupling technique.

4. Validation

To validate the present numerical scheme the results of computational model are compared with correlations proposed by **Shaeri et al.[9]** for large size windows: $\frac{\overline{Nu_{pf}}}{\overline{Nu_{sf}}}=1.296\left(\mathrm{Re}_D\right)^{-0.0352}\left(1-\varphi\right)^{0.269}$ (5)

where ϕ=0.0556 and the ratio of Nusselt number for perforated fin to that of a solid fin $\left(\frac{\overline{Nu_{pf}}}{\overline{Nu_{sf}}}\right)$ have been calculated with respect to different Reynolds number. In order to compare the heat transfer data obtained by the present numerical scheme with the data obtained from the correlations suggested by **Shaeri et al.[9]**, the values of Nusselt number enhancement ratio are plotted as function of Reynolds number. The comparative plot in Fig.3 shows that the present numerical data is in good agreement with the corresponding data found from correlations. The average absolute deviation of the present numerical data from the correlation data is found to be 3.7% which confirms the accuracy of the data.

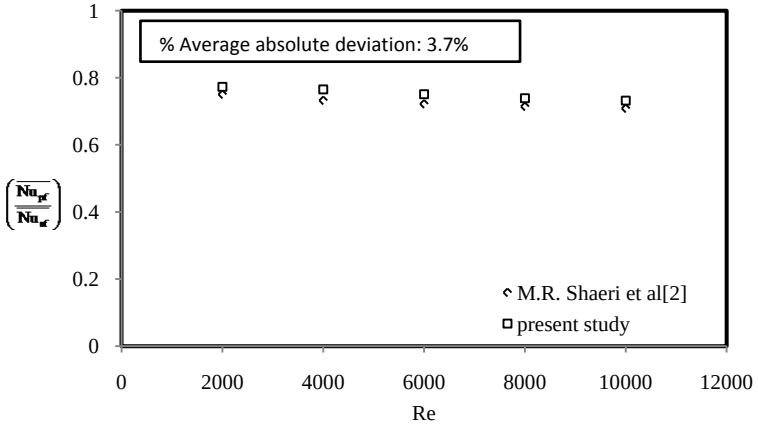

Fig.3: Comparison of present numerical data to Nusselt number enhancement ratio for a perforated fin.

5. Results and discussion

The validated numerical scheme is used to generate the heat transfer and friction data pertaining to the perforated fin under forced convection. The heat transfer and friction characteristics of perforated fin are discussed with the help of plots of heat transfer, Nusselt and friction factor at the fin surfaces as function of fin and operating parameters. The heat transfer performance of perforated fin is also discussed by estimating the heat transfer enhancement due to perforations for different fin configurations while flow Reynolds number is varied from 2000 to 8000. The temperature and velocity counters of solid and perforated fin are discussed to understand the effect of perforation parameters of test fin on heat transfer and friction.

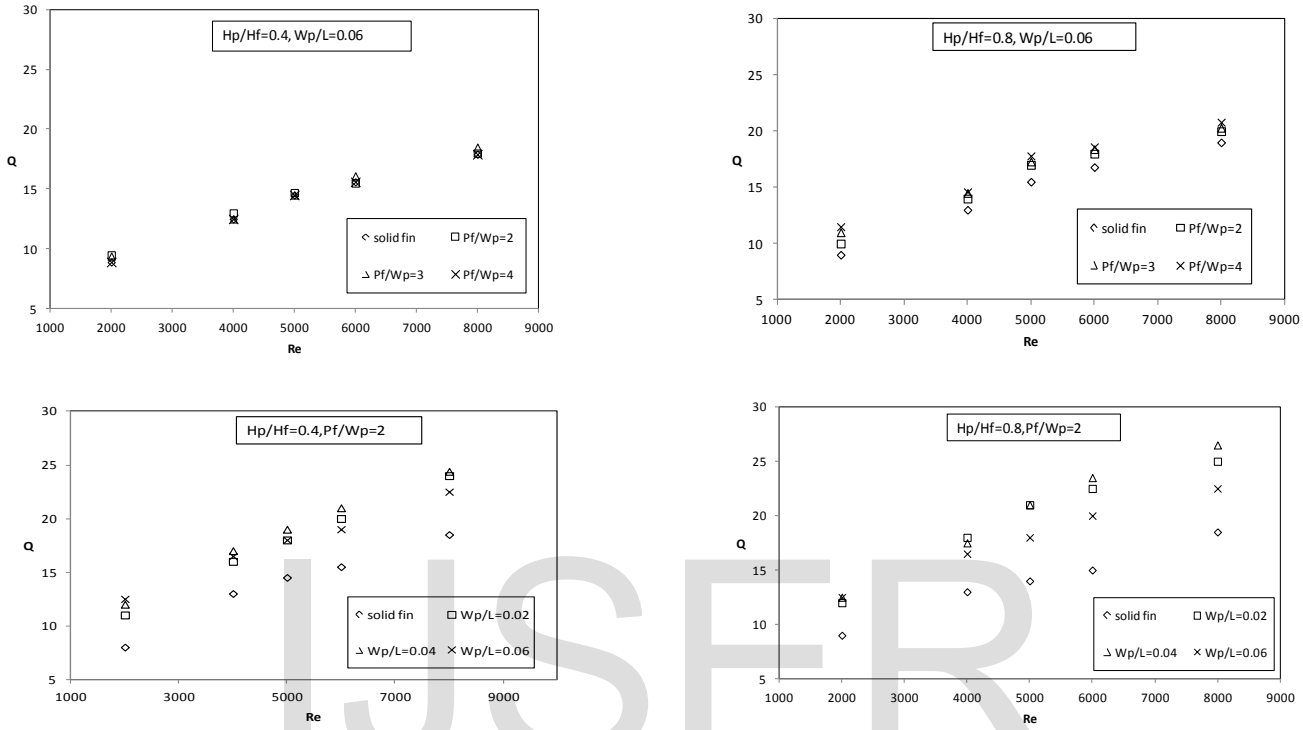

Fig.4: Variation of fin heat transfer rate with Reynolds number for different relative perforation pitch (P_f / W_p) and different relative perforation width (W_p/L).

It is evident that the heat transfer rate from a fin under forced convection is highly sensitive to the fluid flow conditions near the fin surfaces. It is believed that the application of turbulators in the form of perforations promotes disturbance near the wall and thereby yields higher heat transfer rates at the cost of additional pressure drop, Fig.4 shows the plot of fin heat transfer rate as a function of the flow Reynolds number for different relative perforation pitch (P_f /W_p) and relative perforation width (W_p/L) corresponding to two different relative perforation heights (H_p / H_f). It can be observed from the plots that the heat transfer rate increases as the value of Reynolds number is increased for all fin configurations. The plot reveals that the perforated fin yields substantial enhancement in heat transfer than that of a solid fin irrespective of the dimensions of perforation. It can be seen that the heat transfer rates are equally sensitive to the relative perforation width (W_p/L) and relative perforation pitch (P_f /W_p), irrespective of the height of perforation and Reynolds number.

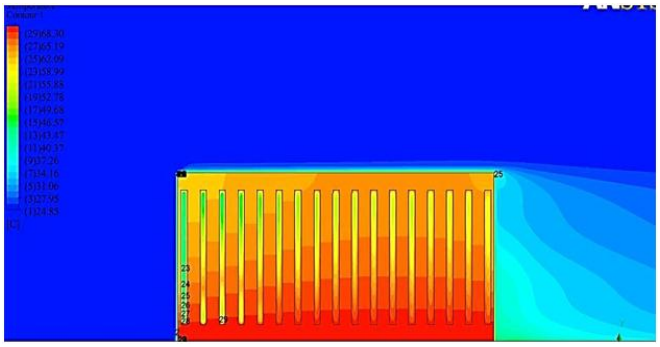

Fig.5. Temperature contour around a fin with perforation at Re=5000 (H_p/H_f=0.8, W_p/L=0.02, P_f/W_p=2).

With a view to understand the heat transfer characteristics of a perforated fin, temperature contours for perforated fin is shown in Fig.5. It can be observed that the temperature of the perforated fin surface towards the leading end is on the lower side when a slot is cut along the length of the fin. This is due to the fact that the cold air stream experiences a higher temperature gradient at the entry section of the slot. As a result of which higher heat transfer rates are achieved near the leading end of the slot. Careful study of temperature contours unfolds that the air stream progresses along the length also helps to flush out the hot air vortices trapped inside the perforations. The accelerated air movement in the perforations leads to better fluid mixing and enhanced heat transfer rates

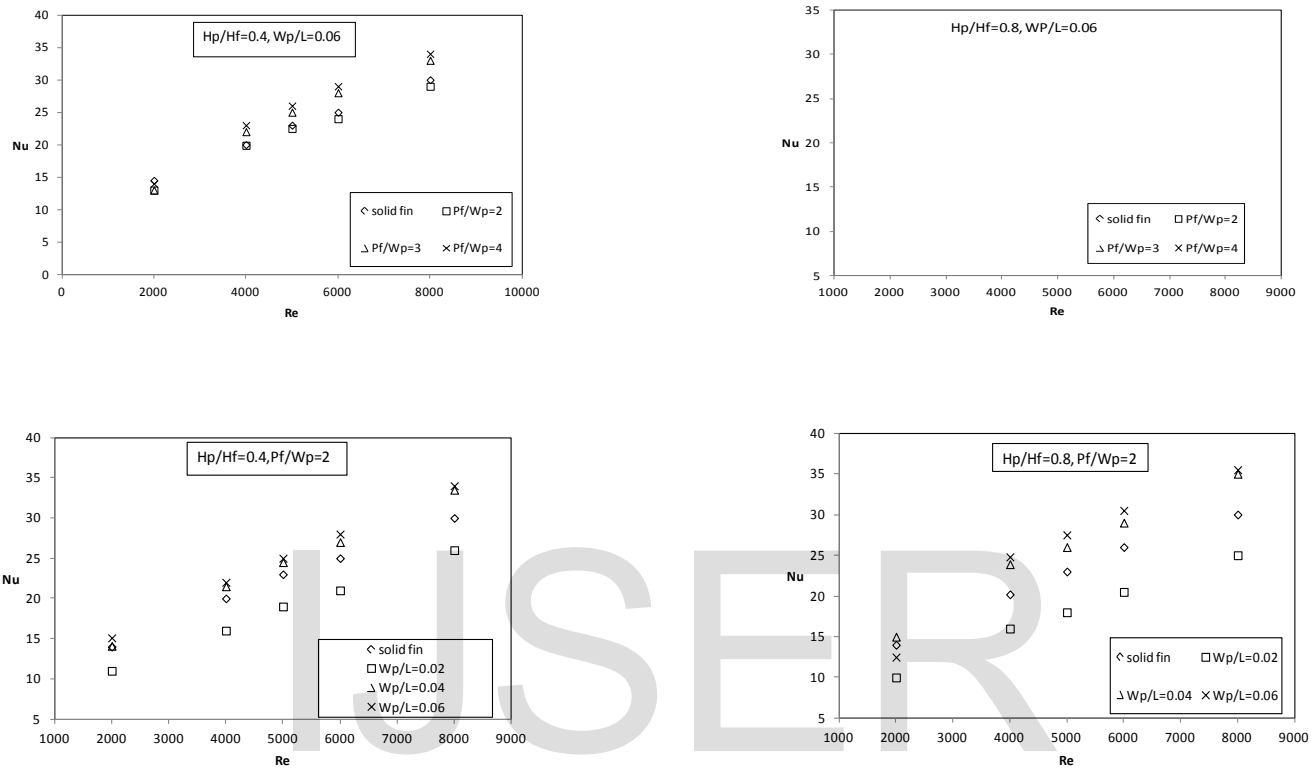

Fig.6. Variation of Nusselt number with Reynolds number for different relative perforation pitch (P_f / W_p) and different relative perforation width (W_p/L).

The relative contribution of heat transfer by convection to that of conduction across the boundary layer developed over the fin surface is usually represented by Nusselt number. To facilitate the understanding of Nusselt number variation over the entire range of Reynolds number, Fig.6 shows the Nusselt number plot for different values of perforation pitch and perforation width. It is interesting to note that the maximum values of Nusselt number are obtained for the perforated fin, followed by the solid fin and perforated fin without slot at all the values of the Reynolds number. It can be noticed that the perforation width has a substantial effect on the Nusselt number at all the values of the flow Reynolds number. The maximum values of Nusselt number are observed at relative perforation pitch (P_f /W_p) of 2, relative perforation width (W_p/L) of 0.06, and relative perforation height (H_p / H_f) of 0.8 irrespective of the values of flow Reynolds number.

Heat transfer enhancements attained by way of turbulence promoters like perforations are usually accompanied by the rise in frictional losses. It is therefore necessary to study the effect of the geometrical parameters of the perforated fin on the friction factor under varied flow Reynolds number. Fig.7 shows the effect of flow Reynolds number on the friction factor with regard to different perforation parameters. The plot shows that the friction factor decreases as the flow Reynolds number is increased for all fin geometries. Notable reduction in friction can be observed for the perforated fin as compared to a solid fin subjected to similar operating conditions. A relatively greater fall in the frictional losses can be observed with the larger height of perforation, at all the Reynolds number. It can be seen that the effect of perforation pitch on friction is insignificant in comparison to the effect of perforation width for both types of fin configurations. Fig.8 the velocity streamlines revealed that the perforated fin has relatively lesser form drag in comparison to the solid fin as the flow confinement within the perforations decreases the length of a recirculation region on the downstream side of the fin and consequently reduces the pressure drop caused by the wake formation.

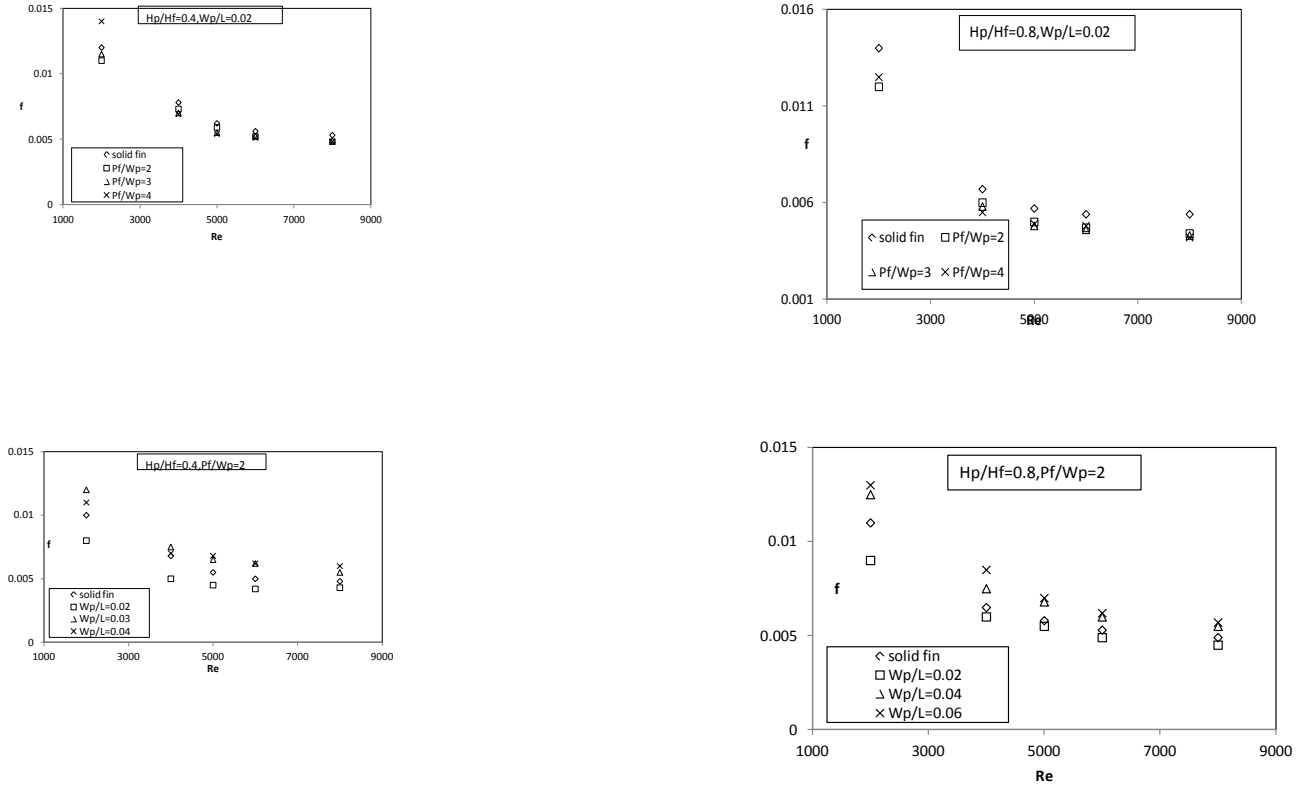

Fig.7. Variation of friction factor with Reynolds number for different relative perforation pitch (P_f / W_p) and different relative perforation width (W_p/L).

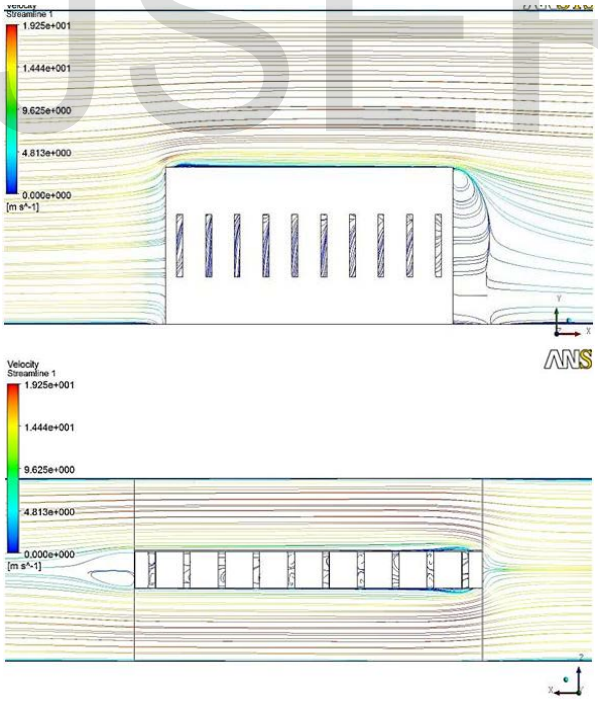

Fig.8. Velocity streamline around a fin without slot, p/Hf=0.4,W_p/L=0.02, Pf/Wp=4 (Re=5000)

6. Conclusions

The present work deals with the study of heat transfer and friction characteristics of a perforated fin by using computational approach.On the basis of present study, following conclusions is drawn:

- The perforated fin has slightly better heat transfer performance with the notable reduction in frictional losses than that of a solid fin.
- The heat transfer increases and friction factor decreases with an increase in the values of Reynolds number for all fin configurations.

- The relative perforation width (W_p / L) of 0.04 has been found suitable for attaining higher heat transfer rates from a perforated fin with relative perforation height (H_p / H_f) of 0.8 whereas relative perforation width (W_p / L) of 0.02 and 0.04 yield comparable heat transfer rates in case of relative perforation height (H_p / H_f) of 0.4.
- The heat transfer rates from perforated fin are intensified when perforation height is increased. However, friction decreases by increasing the height of perforation when perforated fin has no slot.

Nomenclature

A_b	Cross-section area of the base plate
A_f	Cross-section area of the fin
C_p	Specific heat
$C_{p,Al}$	Specific heat of aluminium
D	Fin thickness
D_h	Equivalent hydraulic diameter of duct
f	Friction factor
h	Convective heat-transfer coefficient
h_f	Fin height
h_p	Height of perforation
k_{Al}	Thermal conductivity of aluminium
k	Turbulent kinetic energy
L	Fin length
Nu_s	Nusselt number of solid fin
Nu_{pf}	Nusselt number of perforated fin
Pr	Prandtl number
Q	Heat transfer rate to air
Re	Reynolds number
t	Time
T	Temperature
$T_{in} = T_\infty$	Mean plate temperature
W_p	Width of perforation
$u_{in} = u_\infty$	Inlet velocity of air
X,Y,Z	rectangular coordinate
P/e	Relative rib pitch

Greek symbols

α	Under-relaxation factor
Δ	Difference
μ	Dynamic viscosity
ρ	Density of air at bulk mean air temperature
Φ	General variable
∇	The vector differential operator
ε	turbulent dissipation rate
η	Thermo hydraulic performance

References

[1] Rongguang Jia, Masoud Rokni and Bengt Sunde´n "Impingement cooling in a rib-roughened channel with cross-flow", International Journal of Numerical Methods for Heat & Fluid Flow, Vol. 11; No. 7, pp. 642-662 (2001).

[2] Iaccarino G., Ooi A. and Durbin P.A. , Behnia M. "Conjugate heat transfer predictions in two-dimensional ribbed passages", International Journal of Heat and Fluid Flow, Vol. 23; pp 340–345 (2002).

[3] Meinders E.R, Hanjalic K, Martinuzzi R.J, "Experimental study of the local convection heat transfer from a wall-mounted cube in turbulent channel flow", J Heat Transfer;121:564–73, (1999).

[4] Ledezma G, Morega AM, Bejan A, "Optimal spacing between pin fins with impinging flow". ASME J Heat Transfer ,118:570–7, (1996).

[5] Torii S, Yang W.J., "Thermal transport phenomena over a slot-perforated flat surface in pulsating free stream". Int J Therm Sci, 41:241–52, (2002).

[6] Sahin, B., Demir, A., "Performance analysis of a heat exchanger having perforated square fins. Appl". Therm. Eng. 28, 621–632, (2008).

[7] Dorignac E, Vullierme J.J, Broussely M, Foulon C, Mokkadem M., "Experimental heat transfer on the windward surface of a perforated flat plate" Int J Therm Sci, 44:885–93, (2005).

[8] M.R. Shaeri, M. Yaghoubi., "Numerical analysis of turbulent convection heat transfer from an array of perforated fins",International Journal of Heat and Fluid Flow 30 218–228, (2009).

[9] Shaeri, M.R., Yaghoubi, M., "Heat transfer analysis of lateral perforated fin heat sinks", Applied Energy 86, 2019–2029, (2009).

[10] Leung C.W, Probert S.D., "Heat exchanger performance: effect of orientation". Appl Energy, 33:35–52, (1989).